Communication

Redox-Mediated Negative Differential Resistance Behavior from Metalloproteins Connected through Carbon Nanotube Nanogap Electrodes

Qun Tang, Hye Kyung Moon, Yoonmi Lee, Seok Min Yoon,
Hyun Jae Song, Hyunseob Lim, and Hee Cheul Choi

J. Am. Chem. Soc., **2007**, 129 (36), 11018-11019• DOI: 10.1021/ja074412k • Publication Date (Web): 21 August 2007

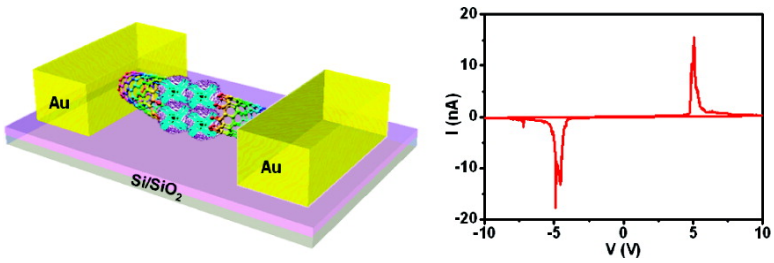

More About This Article

Additional resources and features associated with this article are available within the HTML version:

- Supporting Information
- Links to the 3 articles that cite this article, as of the time of this article download
- Access to high resolution figures
- Links to articles and content related to this article
- Copyright permission to reproduce figures and/or text from this article

View the Full Text HTML

J|A|C|S
COMMUNICATIONS

Published on Web 08/21/2007

Redox-Mediated Negative Differential Resistance Behavior from Metalloproteins Connected through Carbon Nanotube Nanogap Electrodes

Qun Tang, Hye Kyung Moon, Yoonmi Lee, Seok Min Yoon, Hyun Jae Song, Hyunseob Lim, and Hee Cheul Choi*

Department of Chemistry, Pohang University of Science and Technology, San 31, Hyoja-Dong, Nam-Gu, Pohang, Korea, 790-784

Received June 18, 2007; E-mail: choihc@postech.edu

One of the interesting quantum electrical transport phenomena is negative differential resistance (NDR) which has been mostly demonstrated by semiconductor quantum well structures. Recently, similar phenomenon has been realized from various organic molecules including conjugated oligomers[1] and redox-active, species-coupled, self-assembled monolayers (SAMs).[2]

The conventional semiconductor NDR devices are designed to have a planar structure enabling uncomplicated NDR device operation through a simple bias voltage application between two metal electrodes. However, most of the molecular NDR devices are quite restricted by complex measurement systems, for example, scanning probe microscopy in ultrahigh vacuum or at low temperature. To apply such a novel molecular electronic property into practical device applications, it is required to develop planar molecular device systems. Another important issue for the realization of molecular NDR devices is to achieve highly reliable devices. A few examples of the two-terminal planar molecular NDR device generally suffer from severe instability, that is, irrecoverable NDR behavior as they show an almost one-time NDR event upon continuous potential sweep. Here we demonstrate two-terminal planar type molecular NDR devices in which metalloproteins are embedded into electrically cut metallic single walled carbon nanotube (SWNT) electrodes (quasi-one-dimensional electrodes). This device exhibits highly reliable and reproducible NDR behaviors.

The metalloprotein embedded NDR devices were fabricated by locating several ferritin molecules between carbon nanotube nanogap electrodes (gap size: ~20 nm) formed by electrically cutting metallic SWNTs,[3] as described in Figure 1 (see Supporting Information for detailed experimental methods). The driving force for the placement of ferritins inside the nanogap of SWNTs is electrostatic interactions or hydrogen bondings among the residual amino acids of ferritin and carboxylic acid or hydroxyl groups on the circumferences of cut-SWNTs. We found that such a method provided a high probability in locating ferritins with great stability to guarantee reproducible electrical measurements.

A representative NDR behavior from a ferritin−nanogap device is shown in Figure 2a. The ferritin−nanogap device exhibits reproducible NDR behavior upon almost multiple numbers of switching events without signal intensity degradation for 1 month. This particular device showed a NDR peak positioned at 4.90 V with a peak-to-valley ratio (PVR)[4] of ~40 when the bias voltage was swept from 0 to +10 V at the scan rate of 26 mV/s. The peak current density was 4.0×10^6 A·cm^{-2} which is the highest current density reported so far, and the NDR[5] was about -1.2 μohm·cm^2. The ferritin−nanogap device showed hysteresis as no NDR behavior was observed upon the successive sweep in the same bias voltage range regardless of the scan direction (0 to +10 or +10 to 0 V) (Figure 2b). Interestingly, a negative NDR peak was observed when

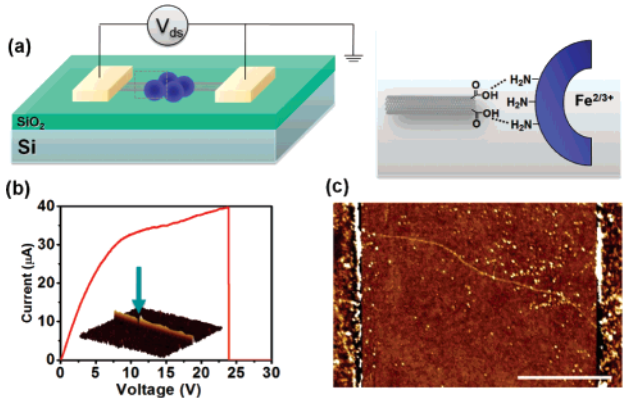

Figure 1. (a) A schematic view of the SWNT-ferritin−SWNT device. A zoom-in view of the dashed box is represented in the right of panel a. (b) $I-V$ curve of cutting metallic SWNT. AFM image of a created nanogap (arrow) having ca. 20 nm gap is shown in the inset. (c) AFM image of a nanotube nanogap device after treating with a ferritin solution (d_{nanotube} = 1.5 nm, scale bar = 1 μm).

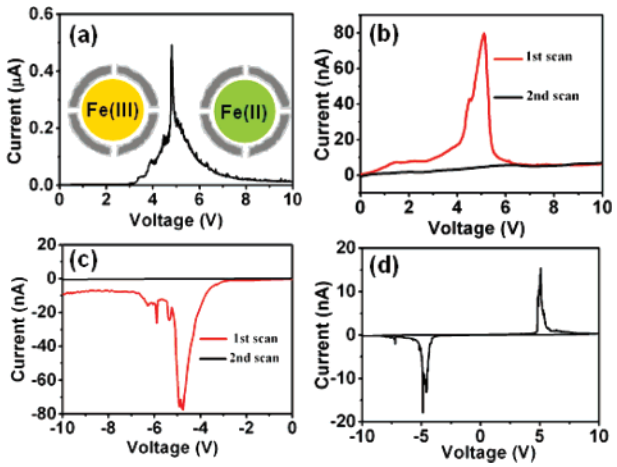

Figure 2. (a) A representative $I-V$ curve of a SWNT-ferritin−SWNT device at room temperature. (b, c) Hysteretic NDR behaviors upon the successive scans from 0 to +10 V and from 0 to −10 V, respectively. (d) A whole $I-V$ cycle sweeping characteristic of the device. The scan was started and ended at 0 V and the scan rate was 53 mV/s.

the device was swept from 0 to −10 V (Figure 2c). After a negative NDR peak was observed, a positive NDR peak reappeared upon the continuous scan up to +10 V.

Thereafter, we confirmed that both NDR peaks could be observed from a full cyclic sweep (0 → +10 → 0 → −10 → 0 V, Figure 2d). Although there were slight variations in NDR peak positions and intensity from device to device, more than 90% of fabricated devices showed similar NDR behaviors. The remaining 10% of devices showed no electrical connection. The $I-V$ curves obtained

10.1021/ja074412k CCC: $37.00

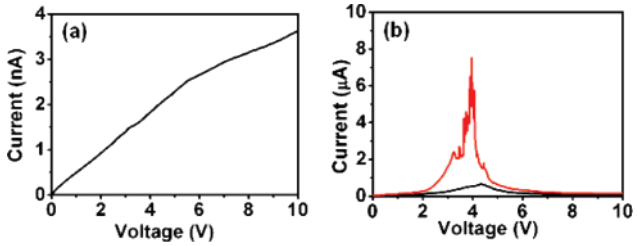

Figure 3. *I*−*V* characteristic curves of (a) apoferritin and (b) artificial ferritins loaded with Fe(III) at the concentrations of 0.25 mM (black curve) and 2.5 mM (red curve).

from 10 different devices and statistical data of PVR, peak current density, and NDR values are listed in Figure S2 and Table S1 (Supporting Information), respectively. Such a high peak current density and high stability seem to be due to the geometrical advantages of the device: the peptide unit of ferritin is a decent electron conductor,[6] which protects the redox active centers securely from environmental attacks. Consequently, unexpected diffusion or dissipation of Fe ionic species is minimized.[7] More importantly, the contact between ferritin and SWNT electrodes might provide ideal interfaces for electron transports, as previously demonstrated by Dai group from pentacene crystals.[3a]

The origin of NDR behavior is due to the reversible electrochemical redox chemistry which involves reduction of Fe(III) ions and oxidation of Fe(II) during the *I*−*V* scan. The reversibility of NDR peak cycles is reminiscent of the behavior of cyclic voltammetry (CV), in which each side of SWNT electrodes is regarded as cathode/anode electrodes, and Fe(III) ions or their clusters are analogous to the electroactive analytes surrounded by peptide dielectric layer. Moistures around the ferritin and nanotube electrodes are believed to play a role as a solvent media which complete an electrochemical system.

To confirm that the NDR behavior from the ferritin−nanogap device indeed originated from a redox species, a series of control experiments were performed. When apoferritins containing no Fe(III) ion in their cores were used, no NDR peak was observed, instead a linear *I*−*V* characteristic curve with high resistance was obtained ($R = 300$ Mohm) (Figure 3a). However, when Fe(III) ions were artificially loaded in apoferritins, NDR peaks were clearly observed (Figure 3b). We further confirmed that the origin of NDR indeed commenced from the Fe species by observing proportionally increased NDR peak current levels as a function of loaded amounts of Fe(III) ions. Next, since the NDR is rooted from the intervalence charge conversion of metal ions, it should behave similarly for other transition metal ions. Among many possible candidates, we examined Co ions since their sizes are appropriate to penetrate into the core of apoferritin. As shown in Figure S1 in the Supporting Information, the Co(III) ion loaded apoferritin device also showed NDR behaviors. Note that all the *I*−*V* characteristic curves slightly deviate from center point, which might come from substrate-caused charge trapping.

The CV-like mechanism for NDR behavior has never been reported from a planar device and is differentiated from previously proposed mechanisms by He[8] and Xiao.[9] Their systems induce NDR because of the irreversible formation of charged species at ferrocenylundecanethiol self-assembled monolayers and irreducible reduction of oligo(phenylene ethynylene)s, respectively. Particularly, these devices showed asymmetric NDR peaks, that is, only one of either positive or negative peak was shown upon a full-scale voltage sweep, while ferritin−nanogap devices showed both NDR peaks upon a full-scale sweep. We should note that there was no significant change in NDR peaks in terms of peak positions and the degree of potential gap between the positive and negative peaks when scanned under N_2 atmosphere or upon scanning at different scan rates. This might be due to the nonclassical redox reaction parameters, such as unique electrochemistry on thin electrodes that could newly rule on carbon nanotube-based nanogap electrodes, which are currently under investigation.

In summary, we demonstrated two-terminal planar type NDR devices from SWNT-ferritin-SWNT nanogap devices that exhibited reproducible NDR peaks with high current density. The NDR behavior roots from active redox reactions of core transition metal ions in ferritin; hence, both positive and negative NDR peaks emerge upon bias voltage sweeps. The SWNT-ferritin−SWNT NDR devices showed much improved characteristics as they were operated under ambient condition and were reliably stable enough to show NDR behaviors upon multiple times of cycles. Electronically active biomolecules trapped between carbon nanotube electrodes might bring greater chances for the realization of potential applications such as logic and memory devices.[10]

Acknowledgment. This work was supported by the Basic Research Program of the KOSEF (R01-2004-000-10210-0), Nano/Bio Science & Technology Program of MOST (2006-00955), SRC/ERC Program (R11-2000-070-070020), and the Korean Research Foundation (MOEHRD, KRF-2005-005-J13103). Profs. Su-Moon Park and Haesik Yang are thanked for helpful discussion.

Supporting Information Available: Complete ref 3c, experimental details, the statistical data of NDR values, an *I*−*V* curve of Co-loaded apoferritin. This material is available free of charge via the Internet at http://pubs.acs.org.

References

(1) (a) Chen, J.; Reed, M. A.; Rawlett, A. M.; Tour, J. M. *Science* **1999**, *286*, 1550. (b) Donhauser, Z. J.; Mantooth, B. A.; Kelly, K. F.; Bumm, L. A.; Monnell, J. D.; Stapleton, J. J.; Price, D. W.; Rawlett, A. M.; Allara, D. L.; Tour, J. M.; Weiss, P. S. *Science* **2001**, *292*, 2303.
(2) (a) Shelly, R.; Snyder, S. R.; White, H. S. *J. Electroanlytical Chem.* **1995**, *394*, 177. (b) Kiehl, R. A.; Le, J. D.; Candra, P.; Hoye, R. C.; Hoye, T. R. *Appl. Phys. Lett.* **2006**, *88*, 172102. (c) Selzer, Y.; Salomom, A.; Ghabboun, J.; Cahen, D. *Angew. Chem., Int. Ed.* **2002**, *41*, 827. (d) Alexei, V.; Tivanski, G.; Walker, C. *J. Am. Chem. Soc.* **2005**, *127*, 7647. (e) Salomon, A.; Arad-Yellin, R.; Shanzer, A.; Karton, A.; Cahen, D. *J. Am. Chem. Soc.* **2004**, *126*, 11648.
(3) (a) Qi, P.; Javey, A.; Rolandi, M.; Wang, Q.; Yenilmez, E.; Dai, H. *J. Am. Chem. Soc.* **2004**, *126*, 11774. (b) Tuukkanen, S.; Toppari, J. J.; Kuzyk, A.; Hirviniemi, L.; Hytonen, V. P.; Ihalainen, T.; Torma, P. *Nano Lett.* **2006**, *6* 1339. (c) Guo, X.; et al. *Science* **2006**, *311*, 356.
(4) PVR was defined by the ratio of the current densities between peak level and a stable level on the OFF state.
(5) Here NDR was defined as the sheet differential resistance of the sharpest slope of *I*(*V*) curve, and the cross-section of a single ferritin is regarded as so-called sheet area instead of the conventional monolayer area.
(6) (a) Zapien, Donald C.; Johnson, Michael A. *J. Electroanal. Chem.* **2000**, *494*, 114. (b) Watt, R. K.; Frankel, R. B; Watt, G. D. *Biochemistry* **1992**, *31*, 9673.
(7) Rajagopalan, V.; Boussaad, S.; Tao, N. J. *Nano Lett.* **2003**, *3*, 851.
(8) He, J.; Lindsay, S. M. *J. Am. Chem. Soc.* **2005**, *127*, 11932.
(9) Xiao, X.; Nagahara, L.; Rawlett, A.; Tao, N. J. *J. Am. Chem. Soc.* **2005**, *127*, 9235.
(10) Reed, M. A.; Chen, J.; Rawlett, A. M.; Price, D. W.; Tour, J. M. *Appl. Phys. Lett.* **2001**, *78*, 3735.

JA074412K